A Novel Series of Selective Agonists Evaluated Against *Rattus Norvegicus* EP_4 Receptor

Holt, Melissa C.[1]; Sidhu, Rana[1]; Ho, Bill[1]; Ciske, Fred L.[1]; Kramer, James B.[1]; Colombo, Joseph M.[1]; Germain, Bradlee D.[1]; Kornilov, Andrei[1]; Uzieblo, Adam[1]; O'Malley, James P.[2]; Owen, Thomas A.[2]; Stein, Adam J.[1]; Morano, M. Ines[1]; Barrett, Stephen D.[1]

[1]Cayman Chemical, 1180 E. Ellsworth Rd., Ann Arbor, MI 48108; [2]Myometrics, LLC, 216 Howard Street, New London, CT 06320

Introduction

Abstract

The EP_4 prostanoid receptor is one of four G protein-coupled receptors (GPCRs) that mediate the actions of prostaglandin E_2 (PGE_2; Item No. 14010). The diverse effects of PGE_2, acting *via* the EP_4 receptor, point to the need to identify novel agonists, both to further elucidate the function of this receptor subtype and for use as therapeutics ranging from bone healing to reducing heart failure. A series of small molecule, EP_4 receptor selective agonists have been generated and evaluated against the *Rattus norvegicus* (rat) homolog. The series includes compounds with picomolar range EC_{50} values as evaluated by Cayman's EP_4 Receptor (rat) Reporter Assay Kit (Item No. 600350), a luminescent cell-based cAMP response element reporter assay. Compounds were counter screened for selectivity against Cayman's EP_2 Receptor (rat) Reporter Assay Kit (Item No. 600340). Compounds were evaluated further by docking onto the rat EP_4 receptor model using Autodock and Schrödinger. These stereoisomerically pure compounds represent a novel set of EP_4 receptor-selective agonists featuring a lactam core, a fully saturated heptanoic acid α-chain, and a unique alkyne ω-chain. Difluoro substitution *alpha* to the lactam ring carbonyl group increased potency more than 5-fold within the SAR study.

Background

Prostaglandin E_2 (PGE_2) in humans is an almost ubiquitous arachidonic acid-COX cascade product that mainly mediates its multitude of signaling roles through activation of the GPCR superfamily-member E-type prostanoid receptors 1-4 (EP_{1-4}) receptors. The roles of functionally related EP_4 and EP_2 receptors have been widely investigated, and the receptors have been considered as therapeutic targets for a variety of indications including cancer, asthma, inflammation, heart failure, colitis, ischemia, and osteoporosis. Selective EP_4 and EP_2 modulators have been sought to provide the benefits of target modulation while limiting side effects arising from the modulation of the other receptor subtypes. Both EP_4 and EP_2 are coupled to G protein-dependent pathways through $G\alpha_s$ and, thus, activate adenylate cyclase and induce synthesis of intracellular cAMP.[1] Though EP_4 and EP_2 share overlapping functional roles, where they both are expressed in bone with roles in bone metabolism, they have only 38% homology in humans and are not pharmacologically identical.[2] It is reasonable to target highly EP_4 receptor selective compounds as therapeutic agents.[3,4]

Roche reported a potent γ-lactam EP_4 receptor agonist, Compound 31, referred to here as CAY10684 (Cayman Item No. 15966).[5] This compound displayed essentially no binding affinity for EP_2. The reported SAR suggested that replacing the PGE_2 ω-chain pentyl terminus with an aromatic ring exploited some difference between the EP_4 and EP_2 binding sites leading to the observed selectivity. Docking studies illustrate the fit and key binding interactions of CAY10684 within EP_4 and EP_2 binding site amino acid residues. Herein, we describe a Cayman SAR series focused on ω-chain substitutions, utilizing an alkyne to provide rigidity. Additionally, the identification of the beneficial *bis*-fluorination of the γ-lactam greatly improved affinity. This work led to KMN-159, a novel, potent, soluble EP_4-selective agonist. Furthermore, we suggest its likely binding mechanism through docking studies which align well with the SAR series, focusing on the benefits of the *bis*-flourination on the improved docking of KMN-159 over KMN-80 (Cayman Item No. 15435).

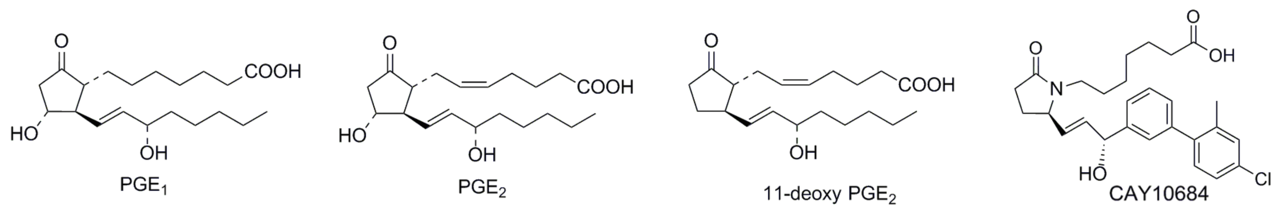

COOH
HO
OH
PGE1
PGE2
11-deoxy PGE2
OH
N
HO
CAY10684
Cl

Figure 1 – Select EP_4 receptor agonists

Methods

Rat EP_4 Receptor Reporter Assay

A batch of frozen HEK293T cells were prepared and stored in vapor phase of a liquid nitrogen vessel. Aliquot(s) of frozen HEK293T/17 cells were thawed and seeded onto a T150 tissue culture flask to allow recovery for 20-24 hours. Cells were harvested from the flasks and re-seeded on an EP_4 reporter assay plate (Cayman Item No. 600350) at a density of 65,000-75,000 cells/well in 200 µL reduced serum medium containing 0.5% FBS. Cells were incubated at 37°C with 5% CO_2 for 16-18 hours to allow expression of the receptor target. Culture media was aspirated and replenished with 100 µL serum-free culture medium. Test compounds were prepared at 2x final concentration and added to wells. For each compound, a 12-point dose-response curve (DRC) in 4-fold serial dilution was performed in triplicate. PGE_2 DRCs were run in parallel in all experiments (concentrations from 0-10 nM). After 6 hours of stimulation, 10 µL of media was transferred to a corresponding well of a 96-well solid white plate. The plate was heated at 65°C for 30 minutes to inactivate endogenous alkaline phosphatase. Luminescence-based alkaline phosphatase substrate (Cayman Item No. 600183) was added to each well and Secreted Embryonic Alkaline Phosphatase (SEAP) activity was measured by reading the luminescence signal after a 10 minute incubation. The EC_{50} values for PGE_2 and each test compound were calculated using GraphPad Prism 6 (GraphPad Prism version 6.00 for Windows, GraphPad Software, La Jolla California USA, www.graphpad.com). The methodology was performed with appropriate substitutions for assaying against rat EP_2 receptor.

Rat EP_4 Receptor and Rat EP_2 Receptor Homology Modeling[6]

The sequences for *R. norvegicus* EP_2 receptor and *R. norvegicus* EP_4 receptor were submitted to RaptorX structure prediction suite (http://raptorx.uchicago.edu/) and analyzed to confirm the quality of the model using the P-value, global distance test, absolute global quality, and RMSD. All metrics indicated the models were acceptable. RaptorX utilized squid and human rhodopsin as the primary templates for rat EP_4 threading and squid rhodopsin and rat neurotensin receptor 1 as the primary templates for rat EP_2 threading. For rEP_4, residues 1-16, 201-288, 352-488 were identified as potentially disordered. For rEP_2, residues 1-17, 52-64, 227-257, 324-357 were identified as potentially disordered. For both models, these regions largely consist of loops. The receptors were prepared for docking in Autodock with MGL Tools 1.5.7.

Rigid and Flexible Docking in Autodock Vina[7]

Ligand 3D PDB files were generated utilizing CACTUS SMILES translator (http://cactus.nci.nih.gov/) and the ligands were prepared with MGL Tools 1.5.7. Rotatable bonds were introduced, amide bonds were held as fixed, and hydrogens were added. A search grid of 27,000 Å^3 centered on residue TYR188 with maximum exhaustiveness was used to dock ligands in rigid mode utilizing Autodock Vina and the AMBER forcefield. Residues lining the various regions of the rigid binding-site were selected and prepared as flexible residues using MGL Tools 1.5.7. Rotatable bonds were introduced, amide bonds were held as fixed, and hydrogens were added. Flexible residues in rEP_4 receptor were PHE28, PHE102, ASN164, SER185, TYR188, SER193, SER288, and ASP314. The same search grid as the rigid docking was used to search with maximum exhaustiveness to dock ligands in flexible mode utilizing Autodock Vina. Ten poses per docking experiment were generated. Poses were evaluated by their score (kcal/mol), how often similar poses repeated, and consistency among multiple models. We sought out trends that were verified within multiple models and consistent with trends observed within cell-based data.

Induced Fit Docking with Schrödinger Maestro 11[8-13]

All files were prepared and generated within Maestro 11. Ligands were prepared with LIGPREP from SMILES using OPLS3 force field modified using EPIK. Molecules were desalted and featured all possible tautomers. Receptors were modified using Maestro Protein Preparation Wizard selecting default values. Positions of hydrogen bonds and torsion angles were refined prior to initiation. A search grid of 8,000 Å^3 was centered on residue TYR188 for rEP_4 receptor docking. A search grid of 8,000 Å^3 was centered on residue SER121 for rEP_2 receptor docking. GLIDE docking was performed and subsequently refined with PRIME to introduce residue flexibility within 5 Å of the binding site. Compounds were evaluated based on docking score, emodel score, and glide score.

Results

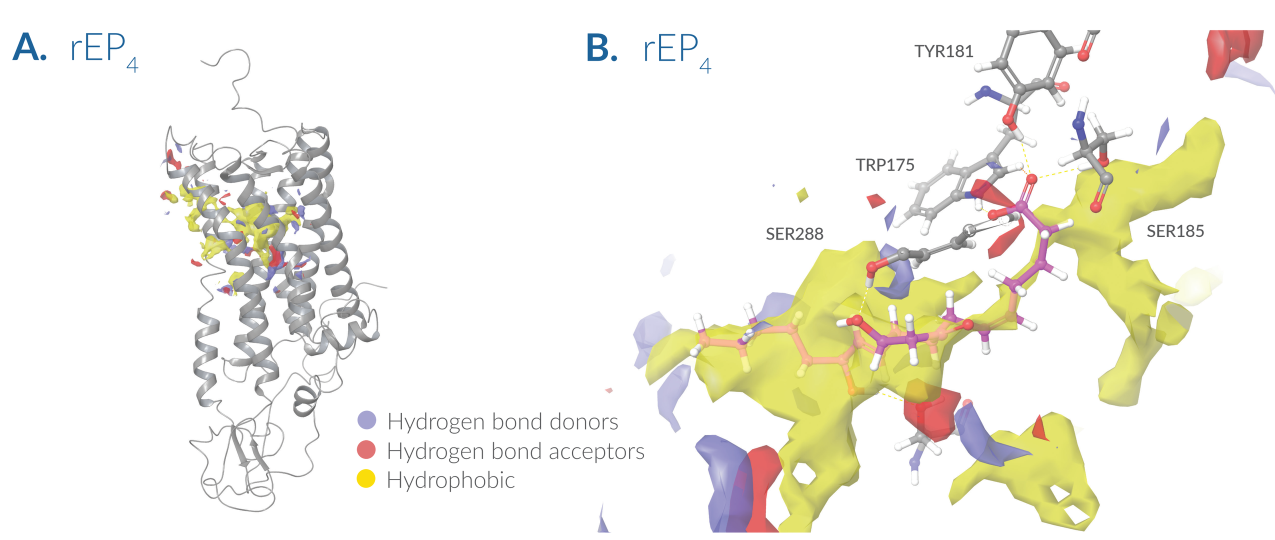

A. rEP4
B. rEP4
TYR181
TRP175
SER288
SER185
Hydrogen bond donors
Hydrogen bond acceptors
Hydrophobic

Figure 2 – A. RaptorX model of Rat EP_4 receptor with proposed ligand binding site identified and highlighted by Maestro 11 Ligand Site. B. Docking of PGE_2 into rEP_4 receptor model using a Maestro Induced Fit model, highlighting key interactions between the α-chain carboxylate with TYR181 and TRP175, 15-hydroxyl with SER288, and 11-hydroxyl with TYR188. Side chains are displayed in gray.

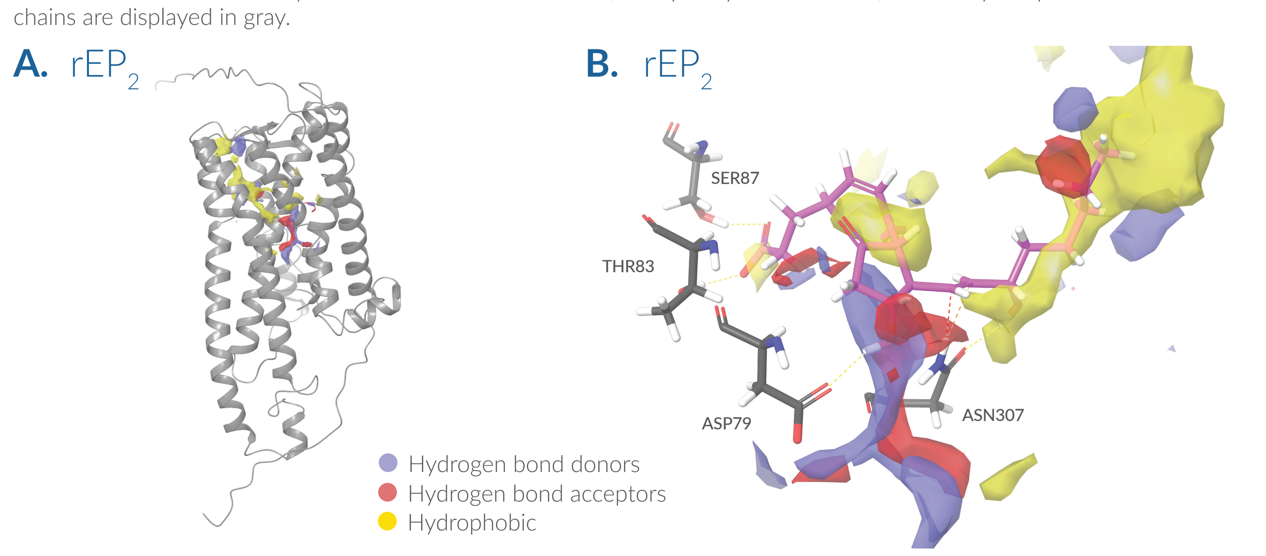

A. rEP2
B. rEP2
SER87
THR83
ASP79
ASN307
Hydrogen bond donors
Hydrogen bond acceptors
Hydrophobic

Figure 3 – A. RaptorX model of Rat EP_2 receptor with proposed ligand binding site identified and highlighted by Maestro 11 Ligand Site. B. Docking of PGE_2 into rEP_2 receptor model using a Maestro Induced Fit model, highlighting key interactions between the 11-hydroxyl with ASP79, α-chain carboxylate with SER87 and THR83, and 15-hydroxyl with ASN307. Side chains are displayed in gray.

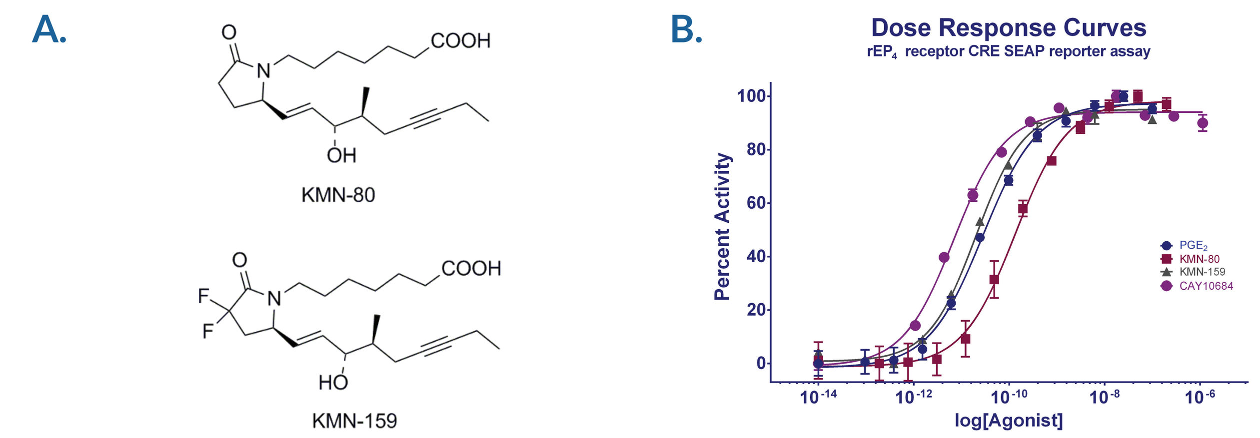

A.
COOH
N
OH
KMN-80
F
HO
KMN-159
B.
Dose Response Curves
rEP4 receptor CRE SEAP reporter assay
Percent Activity
log[Agonist]
PGE2
KMN-80
KMN-159
CAY10684

Figure 4 – A. Structures of KMN-80 and KMN-159. B. Representative data from rEP_4 receptor CRE SEAP reporter assay displaying dose-response curves for PGE_2, KMN-80, KMN-159, and CAY10684.

Compound	EC_{50} (pM) rEP_4R	EC_{50} (nM) rEP_2R	RATIO EP_2/EP_4	rEP_4R AUTODOCK RIGID (kcal/mol)	rEP_2R AUTODOCK RIGID (kcal/mol)	rEP_4R AUTODOCK FLEXRES (kcal/mol)	rEP_4R MAESTRO INDUCED FIT (kcal/mol)	rEP_4R MAESTRO EMODEL	rEP_2R MAESTRO INDUCED FIT (kcal/mol)	rEP_2R MAESTRO EMODEL
PGE_1	21.3±3.6 (n=3)	4.4±0.4 (n=3)	206	-7.7	-6.9	-7.5	-10.72	-99.15	-11.08	-101.1
PGE_2	29.2±1.5 (n=56)	3.3 (n=16)	113	-7.9	-6.9	-8.5	-10.50	-99.2	-11.10	-113.72
11-DEOXY PGE_2	36.9±10.7 (n=6)	38.71±4.48	1,049	-7.9	-7.3	-8	-9.77	-87.83	-10.58	-83.83
CAY10684	6.9±0.06 (n=3)	>5,000	>724,637	-8.9	-5.7	-9.7	-14.72	-149.97	-13.01	-116.56
KMN-159	26.5±2.7 (n=7)	4,900	184,905	-8.4	-6.3	-8.3	-11.81	-111.93	-11.21	-94.74
KMN-80	166.61±14 (n=6)	>10,000	>60,000	-7.7	-6.8	-7.9	-11.23	-103.06	-10.98	-94.47

Table 1 – Compiled data from rEP_4 receptor CRE SEAP reporter assay, rEP_2 receptor CRE SEAP reporter assay counter screen, Autodock docking studies, and Schrödinger docking studies.

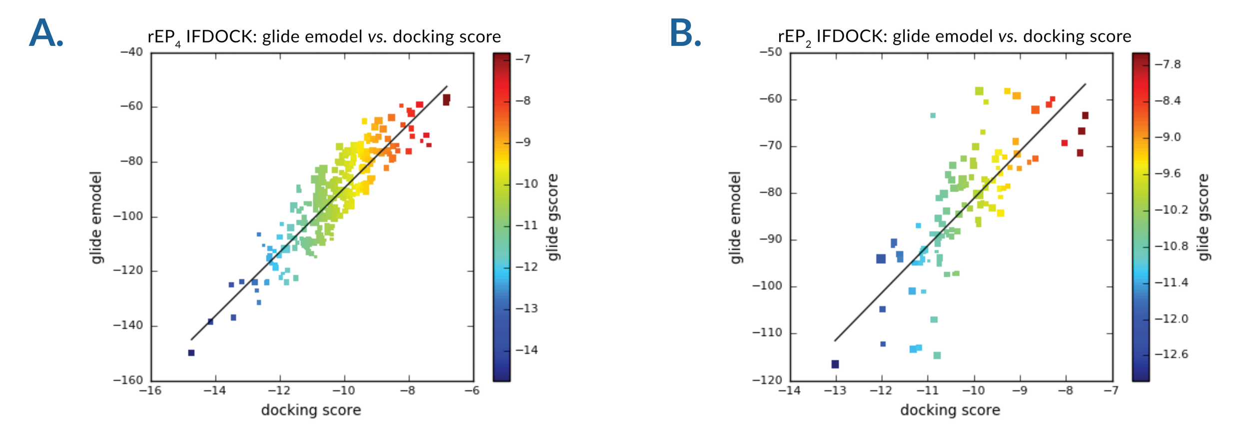

A.
rEP4 IFDOCK: glide emodel vs. docking score
glide emodel
docking score
glide gscore
B.
rEP2 IFDOCK: glide emodel vs. docking score
glide emodel
docking score
glide gscore

Figure 5 – A. Plot of docking score (kcal/mol) *versus* emodel score for compounds docked against rEP_4 receptor. B. Emodel score *versus* docking score for ligands docked against rEP_2. Poses with higher internal strain display higher emodel scores and are ranked lower than poses with low emodel scores (more negative). All data points are colored based on glide gscore, a metric similar to docking score. The points are sized according to their glide einternal score, a measure of torsional strain, where smaller indicates less strain.

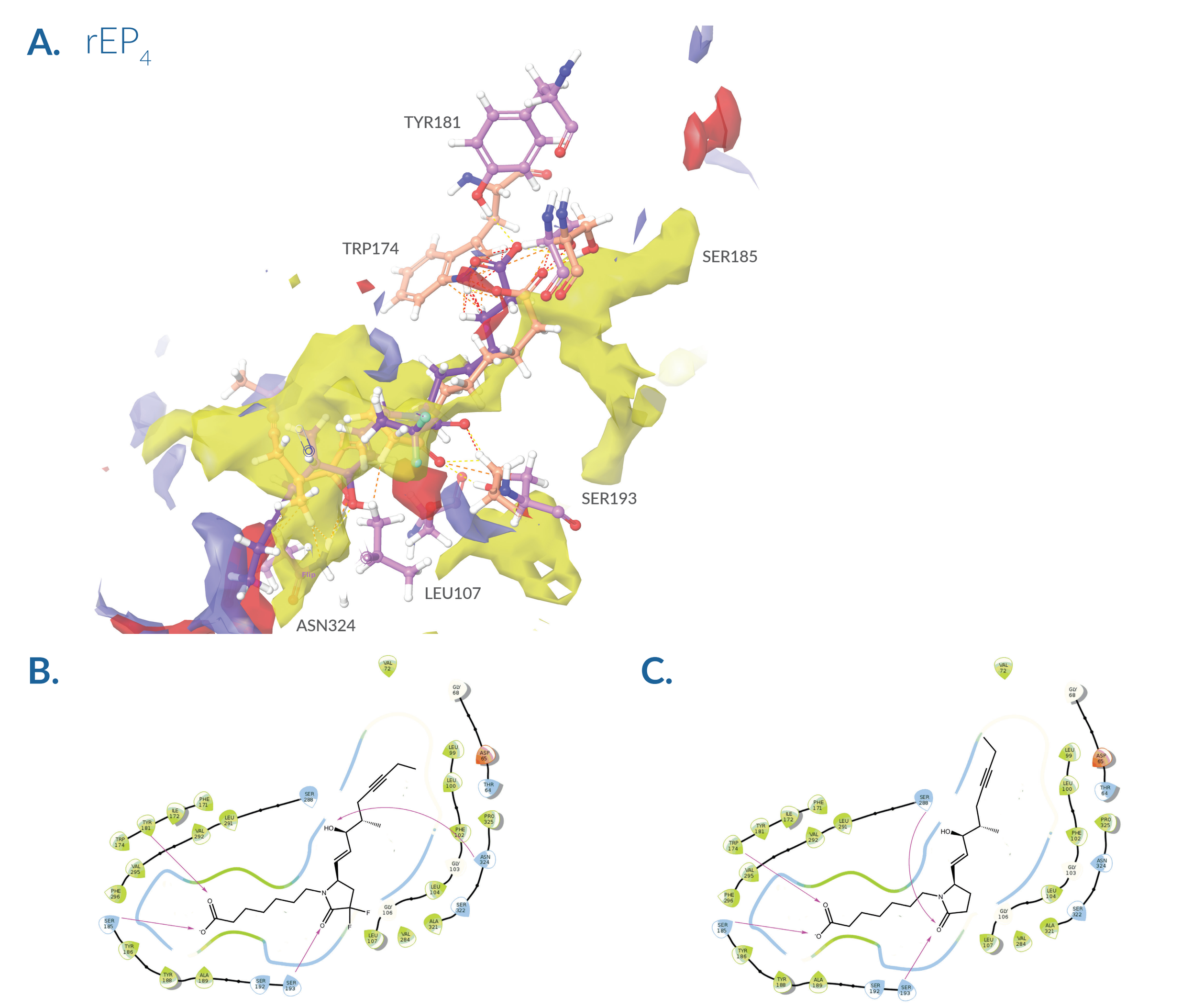

A. rEP4
TYR181
TRP174
SER185
SER193
LEU107
ASN324
B.
C.

Figure 6 – A. Compound overlay of KMN-159, and KMN-80 to rEP_4 receptor generated from Maestro 11 Induced Fit model featuring site map. Side chains for each flexible dock are shown in either pale pink or pale orange. B. Key interactions for KMN-159 in 2D plot. C. Key interactions for KMN-80 in 2D plot.

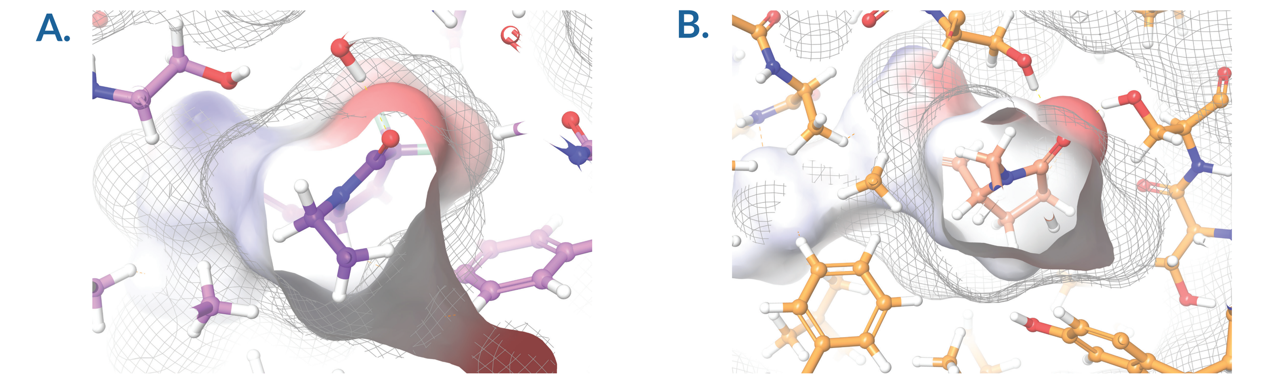

A.
B.

Figure 7 – A. Top docking pose of KMN-159 rEP_4 receptor generated from Maestro 11 Induced Fit model featuring surface representation of receptor and ligand binding site. B. Top docking pose of KMN-80 rEP_4 receptor generated from Maestro 11 Induced Fit model featuring surface representation of receptor and ligand binding site.

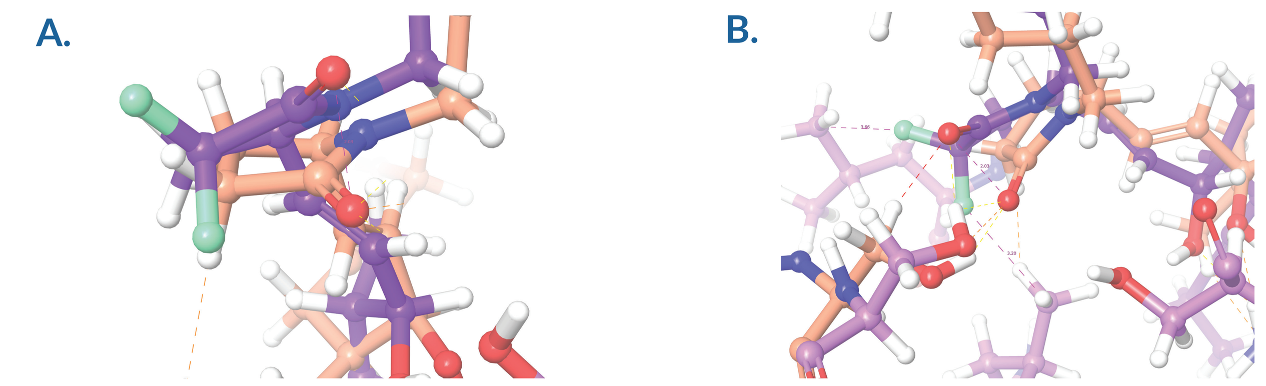

A.
B.

Figure 8 – A. Zoom in of puckered KMN-80 ring. B. Zoom in of flat KMN-159 ring.

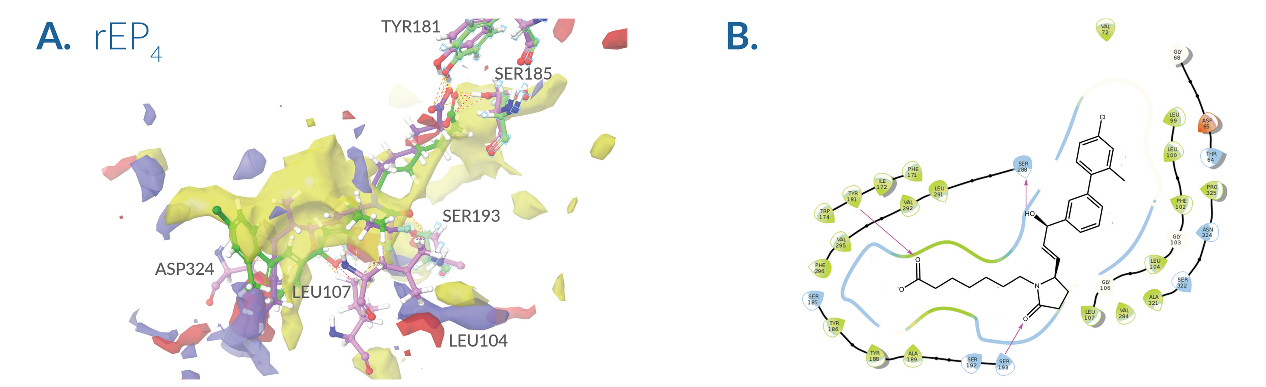

A. rEP4
TYR181
SER185
SER193
ASP324
LEU107
LEU104
B.

Figure 9 – A. Compound overlay of KMN-159 and CAY10684 featuring site map. Side chains for each flexible dock are shown in either pale pink or pale green. B. Key interactions of CAY10684 in 2D plot.


A. rEP2
SER87
THR83
ASP79
ASN307
B. rEP2
SER87
THR83
ASP79
ASN307

Figure 10 – A. Binding mode of PGE_2 with overlay of KMN-159 in rEP_2 Maestro 11 Induced Fit model featuring site map. Note that KMN-159 does not sit in bottom of pocket like PGE_2. Side chains forming PGE_2 binding pocket are ASP79, THR83, SER87, and ASN307 (gray). ASN307 makes a polar contact with KMN-159 carboxylate. B. Binding mode of PGE_2 with overlay of CAY10684 in rEP_2 Maestro 11 Induced Fit model featuring site map. Note that CAY10684 does not overlap well and displays high internal torsion metrics.

Conclusions

Key interactions were highlighted from this docking study regarding the binding of a series of novel rEP_4 receptor agonists. The lactam carbonyl is seen interacting with SER193 in nearly all compounds. A large hydrophobic pocket has been identified, which likely could be further exploited in the KMN series. SER185 is seen commonly locking the α-chain carboxylate into place. Additionally, TYR181 and TRP174 are seen as interacting with the α-chain carboxylate in some cases and not others. The 15-hydroxyl displayed the greatest variability and sensitivity in its interactions. In the case of KMN-80 *versus* KMN-159, we postulate that the increased size of the difluoro, coupled with the conformationally locked, flat nature of the 159 γ-lactam, shifts the docked position of KMN-159 to make a more favorable hydrogen bonding interaction with the 15-hydroxyl relative to KMN-80 at a lower entropic cost. The increased potency of KMN-159 is a result of the interaction of the 15-hydroxyl with ASN324 and coordination of LEU104 and LEU107 by the difluoro moiety. These beneficial interactions are not present in KMN-80. KMN-159 displayed a very similar binding mode relative to CAY10684. CAY10684 displayed very strong metrics within the binding experiment. Additionally, compounds docked against the rEP_2 receptor displayed poorer metrics and did not overlay well with the natural substrates, particularly PGE_2. These docking studies have allowed the interpretation of the SAR work in greater detail. The addition of the difluoro moiety is thought to play a small steric role, shifting the position of the lactam ring slightly, conformationally locking the γ-lactam, and improving the coordination of the carboxylate and 15-hydroxyl with their associated binding niches.

References

1. Sugimoto, Y. and Narumiya, S. *J. Biol. Chem.* **282(16)**, 11613-11617 (2007).
2. Blackwell, K.A., Raisz, L.G., and Pilbeam, C.C. *Trends Endocrinol. Metab.* **21(5)**, 294-301 (2010).
3. Ke, H.Z., Crawford, D.T., Qi, H., *et al. J. Bone Miner. Res.* **21(4)**, 565-575 (2006).
4. Weinreb, M. and Shir, G.N. *Am. J. Physiol. Endocrinol. Metab.* **276(2)**, E376-E383 (1999).
5. Elworthy, T.R., Kertesz, D.J., Kim, W., *et al. Bioorg. Med. Chem. Lett.* **14(7)**, 1655-1659 (2004).
6. Källberg, M., Wang, H., Wang, S., *et al. Nat. Protoc.* **7**, 1511-1522 (2012).
7. Seeliger, D. and de Groot, B.L. *J. Comput. Aided Mol. Des.* **24(5)**, 417-422 (2010).
8. Friesner, R.A., Murphy, R.B., Repasky, M.P., *et al. J. Med. Chem.* **49(21)**, 6177–6196 (2006).
9. Halgren, T.A., Murphy, R.B., Friesner, R.A., *et al. J. Med. Chem.* **47(7)**, 1750–1759 (2004).
10. Friesner, R.A., Banks, J.L., Murphy, R.B., *et al. J. Med. Chem.* **47(7)**, 1739–1749 (2004).
11. Farid, R., Day, T., Friesner, R.A., *et al. Bioorg. Med. Chem.* **14(9)**, 3160-3173 (2006).
12. Sherman, W., Day, T., Jacobson, M.P., *et al. J. Med. Chem.* **49(2)**, 534-553 (2006).
13. Sherman, W., Beard, H.S., and Farid, R. *Chem. Biol. Drug Des.* **67(1)**, 83-84 (2006).